Evolution of Microstructure and Transport Properties of Cement Pastes Due to Carbonation under a CO_2 Pressure Gradient—A Modeling Approach

Q. T. Phung[1,2,a]; N. Maes[2,b]; D. Jacques[2,c]; G. De Schutter[1,d]; and G. Ye [1,3,e]

[1]Magnel Laboratory for Concrete Research, Ghent University, B9052 Ghent, Belgium. E-mail: [a]QuocTri.Phung@sckcen.be; [d]Geert.DeSchutter@ugent.be
[2]EHS Institute, Belgian Nuclear Research Centre (SCK•CEN), Boeretang 200, B2400 Mol, Belgium. E-mail: [b]Norbert.Maes@sckcen.be; [c]Diederik.Jacques@sckcen.be
[3]Microlab, Delft University of Technology, P.O. Box 5048, 2600 GA Delft, The Netherlands. E-mail: [e]G.Ye@tudelft.nl

Abstract

Most carbonation models only account for diffusion as the main transport mechanism rather than advection. Nevertheless, in the case of concrete used for underground waste disposal facilities, concrete may be subjected to a high hydrostatic pressure and the surrounding environment may contain a high dissolved CO_2 concentration. Therefore, a combination of diffusion and advection should be taken into account. This is also the case in accelerated carbonation where a high CO_2 pressure gradient is applied in which advection in the gas phase has a significant contribution to the carbonation process. This study aims at developing a model to predict the evolution of the microstructure and transport properties of cement pastes due to carbonation under accelerated conditions in which a pressure gradient of pure CO_2 is applied. The proposed model is based on a macroscopic mass balance for carbon dioxide in gaseous and aqueous phases. Besides the prediction of the changes in transport properties (diffusivity, permeability), the model also enables to predict the changes in microstructure. Data from accelerated tests were used to validate the model. Preliminary verification with experimental results shows a good agreement.

1. INTRODUCTION

The carbonation process in cement-based materials is a deterioration phenomenon. Carbonation results in a pH decrease. The development of lower alkaline environment accelerates the corrosion of reinforcing bars in concrete because of dissolution of the thin oxide passive layer protecting the steel bars from corrosion (Glasser et al. 2008). On the other hand, carbonation also results in beneficial effects. It is generally believed that carbonation decreases transport properties and refines pore structure of Portland cement-based materials. However the extent of modification in transport properties and microstructure significantly depends on carbonation conditions and cement types. The reduction of transport properties is the result of the precipitation of carbonation products in the pore structure. This leads to a significant reduction of the total porosity and transport properties.

In general, it is thought that the carbonation mechanism is determined by the inward diffusion of CO_2 in normal conditions. Nevertheless, in the case of concrete used for underground waste disposal purposes, concrete is almost fully saturated and subjected to a high hydrostatic pressure and the surrounding environment may contain a high bicarbonate concentration. Therefore, a combination of diffusion and advection should be taken into account when one considers the carbonation mechanism. However, so far as the authors are aware, none of published studies considers the contribution of advection to the carbonation modelling.

A number of models have been proposed based on Fick's law for diffusion. Almost all models relate the carbonation depth with square root of time. However, a sharp front is not always observed. Instead of giving an explicit formula to predict the carbonation depth, a large number of models have been developed in order to solve the carbonation problem numerically (Bary and Sellier 2004; Muntean et al. 2011). These approaches are mainly based on conservation laws and can capture most important factors influencing the carbonation process. As carbonation of cement-based materials under atmospheric conditions is a slow process; a number of accelerated carbonation methods have been proposed. A common way is to put concrete samples in a controlled chamber with a specific CO_2 partial pressure and an optimized relative humidity (50-70%) to speed up carbonation. An alternative method has been proposed in a companion paper (Phung et al. 2015) in which a high pressure gradient of pure CO_2 is applied to samples at controlled initial internal relative humidity. Interpretation of such accelerated carbonation experiment requires a 1-D reactive transport model accounting for advective flow as a consequence of the applied CO_2 pressure gradients. Contrary to the existing models, the proposed model accounts for both advective and diffusive transports. Besides the prediction of the carbonation depth, the model also enabled to predict the change in permeability, diffusivity, and porosity due to carbonation.

2. MODEL DEVELOPMENT

The proposed model was based on a macroscopic mass balance for CO_2 in gaseous and aqueous phases. A simplified solid-liquid equilibrium curve was used to relate the Ca contents in aqueous and solid phases. The model only considers the carbonation of portlandite (CH) and calcium silicate hydrates (C-S-H). Initial hygrothermal conditions were accounted for and their evolutions during carbonation are also considered. It is assumed that the hydration of concrete is not changed when the carbonation process starts.

2.1. Theory

2.1.1. Mass conservation of CO_2

The mass balance equation for CO_2 is given as:

$$\partial c/\partial t + \partial J/\partial x = -Q \tag{1}$$

where c is the total concentration of CO_2 in the porous media [kg/m^3]; J is the total flux of CO_2 [kg/m^2.s]; Q is the reaction rate of CO_2 [kg/m^3.s], t is time [s] and x is the spatial distance [m]. The total concentration of CO_2 in the porous media is the sum of the amounts of CO_2 in the gaseous c_g and aqueous c_l phases [kg/m^3]:

$$c = \phi(1-S)c_g + \phi S c_l \tag{2}$$

where ϕ is porosity [-] and S is water saturation degree [-]. The total flux of CO_2 includes both the CO_2 fluxes in the gaseous J_g and aqueous J_l phases. Accounting for diffusion and advection results in following equation:

$$J = J_g + J_l = -\left[c_g v_g + D_g(\partial c_g/\partial x)\right] - \left[c_l v_l + D_l(\partial c_l/\partial x)\right] \tag{3}$$

where D_g and D_l are effective diffusion coefficients of gaseous and aqueous phase, respectively [m^2/s]; v_g and v_l are the volumetric flux densities [m/s] of gaseous and aqueous phases due to a pressure gradient, respectively, which are obtained via Darcy's law for the aqueous and gaseous phases as:

$$v_l = -(k_l(\phi,S)/\mu_{H_2O})(\partial P_l/\partial x) \qquad k_l(\phi,S) = k_{l0}(\phi)k_l(S) \tag{4}$$

$$v_g = -(k_g(\phi,S)\beta(P_a)/\mu_{CO_2})(\partial P_g/\partial x) \qquad k_g(\phi,S) = k_{g0}(\phi)k_g(S) \tag{5}$$

where μ_{H_2O} and μ_{CO_2} denote the dynamic viscosity of water and CO_2 gas, respectively [Pa.s]. $k_{g0/l0}(\phi)$ is intrinsic permeability [m^2] which depends on porosity; and $k_{g/l}(S)$ is the function accounting for the effect of saturation degree on the intrinsic permeability of gaseous/aqueous phase, respectively. P_g and P_l [Pa] denote the pressure of gaseous phase and pore solution, respectively

The relationships between permeability and saturation degree are expressed by invoking the relation of (van Genuchten 1980) and (Wardeh and Perrin 2006) for the aqueous and gaseous phases, respectively:

$$k_l(S) = S^p\left[1-(1-S^{1/q})^q\right]^2 \qquad k_g(S) = (1-S)^p\left(1-S^{1/q}\right)^{2q} \tag{6}$$

where p [-] and q [-] are empirical coefficients. In order to establish the relationship between permeability and pore structural parameters, we explored well-known Kozeny-Carman relation.

$$k = \chi\phi^3/(1-\phi)^2 \qquad \chi = \left(\tau^2 S_a^2 F_s\right)^{-1} \tag{7}$$

where χ [m^2] is a function of tortuosity, τ [-]; specific surface of pores, S_a [m^2/m^3]; and shape factor, F_s [-]. Both parameters τ and F_s are very difficult to quantify because of the complex pore system of hardened cement paste. However, the lumped term $\Omega = 1/\tau^2 F$ [-] can be determined with the knowledge of intrinsic permeability, total porosity and specific surface of pores. Numerical calculation of Ω performed on carbonated and reference samples (Phung et al. 2015) shows that the average value of Ω for sound materials is one order of magnitude higher than one for carbonated materials. Therefore, we assume that the lumped term Ω linearly decreases as a function of carbonation degree as follows:

$$\Omega = \Omega_0 - (\Omega_0 - \Omega_c)d_c = \Omega_0(1-0.9d_c) \tag{8}$$

where subscript 0 and c denote for sound and carbonated materials; Ω_0 can be calculated from porosity, specific surface area and intrinsic permeability of reference sample; d_c is the carbonation degree (see Section 2.2.1).

The $\beta(P_a)$ function is introduced to account for the slip effect on gas permeability known as the Klinkenberg effect and is written as:

$$\beta(P_a) = (1+\lambda/P_a) \tag{9}$$

where λ is a saturation dependent parameter (Abbas et al. 1999) $\lambda = 3.37 - 0.036S$ [atm] and P_a denotes the mean pressure [atm]. We use the empirical formula proposed by (Papadakis et al. 1991) to calculate the diffusivity of gaseous CO_2:

$$D_g = D_0\phi^{1.8}(1-RH)^{2.2} \tag{10}$$

The effective diffusivity calculated in Eq. (10) is actually applied for large pores (molecular diffusion). However, in carbonated/carbonating material, of which the pore size range is shifted to smaller size, Knudsen diffusion should be considered together with molecular diffusion. In this case, the (bulk) effective diffusivity is smaller as reported by (Houst and Wittmann 1994). In a simplified approach, we take into account this effect by changing D_0 to $10^{-d_c}D_0$, and $\phi^{1.8}$ to $\phi^{1.8+k_1 d_c}$, where d_c is the carbonation degree; and k_1 is in range 0.5 – 1. The value of k_1

may be determined if the gas diffusivity of carbonated cement paste is known. For dissolved CO_2, we account for the effects of porosity, tortuosity, and saturation degree as the proposed following equation to estimate effective diffusivity of dissolved CO_2:

$$D_l = D_{l0} \times k_D(\phi,\tau) \times k_D(S) \tag{11}$$

where $k_D(\phi,\tau)$ [-] accounts for the contributions of porosity and tortuosity. This relation was proposed by (Garboczi and Bentz 1992):

$$k_D(\phi,\tau) = 0.001 + 0.07\phi_c^2 + 1.8H(\phi_c - 0.18)(\phi_c - 0.18)^2 \tag{12}$$

where and $H()$ is the Heaviside function; $k_D(S)$ [-] accounts for the effect of saturation degree (Thiéry 2005):

$$k_D(S) = \left(1 + 625(1-S)^4\right)^{-1} \tag{13}$$

Eq. (12) was originally developed for sound materials. As carbonation proceeded, the precipitation of calcium carbonate does not only reduce the porosity but also increase the tortuosity. Therefore, with the same porosity drop, the reduction of diffusivity is expected to be faster for carbonation compared to hydration. Experimental results (Phung 2015) shows that the relative diffusivity of carbonated zone is about 70% smaller than the relative diffusivity of sound material with the sample capillary porosity. As a first estimation, Eq. (13) is adapted for carbonating materials as:

$$k_D^*(\phi,\tau) = \left(1 - 0.7d_c\right)k_D(\phi,\tau) \tag{14}$$

The saturation degree is related to the internal relative humidity by combining Kelvin-Laplace equation and van Genuchtens relation (van Genuchten 1980):

$$S = \left[1 + \left(-\alpha \ln(RH)\right)^{\frac{1}{1-\beta}}\right]^{-\beta} \tag{15}$$

where α and β are experimental fitting parameters.

Evolution of porosity due to carbonation

The change in porosity is estimated by comparing the volume of new products (solid) produced by the carbonation of portlandite and C-S-H.

$$Ca(OH)_2 + CO_2 = CaCO_3 + H_2O \qquad \Delta\phi_{CH} = \left(C_{CH0} - C_{CH}\right)/M_{CH}\left(V_{CH} - V_{CC}\right) \tag{16}$$

y_0CaO•SiO$_2$•z_0H$_2$O + (y_0-y)CO$_2$ = yCaO•SiO$_2$•zH$_2$O + (y_0-y)CaCO$_3$ + (z_0-z)H$_2$O

$$\Delta\phi_{CSH} = C_{CSH0}/M_{CSH0}\left[\left(y_0 - y\right)V_{CC} - \left(V_{CSH0} - V_{CSH}\right)\right] \tag{17}$$

where $\Delta\phi_{CH}$ and $\Delta\phi_{CSH}$ are porosity changes [-] due to portlandite and C-S-H carbonation, respectively; y and z are the average Ca/Si ratio and stoichiometric ratio of H_2O in C-S-H, respectively; C_{CH} and C_{CSH} are portlandite and C-S-H contents [kg/m^3], respectively; M_{CH} and M_{CSH} [kg/mol] are molar masses of portlandite and C-S-H, respectively; V_{CH}, V_{CC} and V_{CSH} [m^3/mol] are molar volumes of portlandite, calcite and C-S-H, respectively. Subscript 0 denotes initial condition. Data for molar volume of C-S-H is still scarce and it is supposed to be stoichiometry-dependent parameter. Recent experimental study (Morandeau et al. 2014) showed that the molar volume of C-S-H is in direct proportion to Ca/Si ratio as:

$$V_{CSH0} - V_{CSH} = \omega\left(1 - y/y_0\right) \tag{18}$$

where $0.02 < \omega < 0.04$ [l/mol]. By comparing the porosity of carbonated and uncarbonated samples, we find that $\omega = 0.04$ [l/mol] gives the best fit. The total porosity of sample during carbonation is simply expressed as follows:

$$\phi = \phi_0 + \Delta\phi_{CH} + \Delta\phi_{CSH} \quad (19)$$

where ϕ_0 is initial total porosity which is determined experimentally or can be calculated as follows (Hansen 1986):

$$\phi_0 = (w/c - 0.17m)/(w/c + 0.32) \quad (20)$$

in which m denotes the degree of hydration. The change in capillary porosity is mainly due to the carbonation of portlandite. However, C-S-H carbonation might partially contribute to the capillary porosity change, especially in accelerated conditions which is expressed by coefficient υ ($0 \le \upsilon \le 1$) as follows. The value of υ is set to be 0.5 in this study, which gives a good fit with capillary porosity change determined by MIP.

$$\phi_c = \phi_{c0} + \Delta\phi_{CH} + \upsilon\Delta\phi_{CSH} \quad (21)$$

where ϕ_{c0} is initial capillary porosity which is either determined by experiment or calculated as follows (Hansen 1986):

$$\phi_0 = (w/c - 0.36m)/(w/c + 0.32) \quad (22)$$

Reaction kinetics

As mentioned before, we only take into account the carbonation of CH and C-S-H. Instead of separately modelling the carbonation reactions of CH and C-S-H, we combine both reactions as a single reaction between Ca^{2+} (dissolved from CH and C-S-H) and CO_3^{2-} ions:

$$Ca^{2+}(\text{total}) + CO_3^{2-} \rightarrow CaCO_3 \quad (23)$$

We consider that the reaction (23) is of the first order with respect to Ca^{2+} and CO_3^{2-}. The rate of the combined carbonation reaction, r [mol/s.m^3], is written as follows:

$$r = -Q/(\phi M_{CO_2}) = -\partial[CH]/\partial t - \partial[C-S-H]/\partial t = k_C f(S) k_r (C_{Ca}/M_{Ca})(C_{CO_3}/M_{CO_3}) \quad (24)$$

where k_C [m^3/mol.s] is the reaction rate coefficient, which is temperature dependent, expressed via the Arrhenius' equation:

$$k_C = \psi.\exp(-E_0/RT) \quad (25)$$

in which ψ is prefactor [m^3/mol.s] and E_0 is activation energy [J/mol]. C_{Ca} and C_{CO_3} [kg/m^3] are total concentration of Ca^{2+} in solution and concentration of CO_3^{2-}, respectively. M_{Ca} and M_{CO3} [kg/mol] are molar masses of Ca^{2+} and CO_3^{2-}, respectively. The concentration of CO_3^{2-} can be related to the concentration of dissolved CO_2 by considering the equilibrium of CO_2 in solution. The function $f(S) = S^n$ (n = 3.7 (Papadakis et al. 1991)) is introduced in Eq. (24) in order to account for the effect of saturation degree on the carbonation reaction rate. The carbonation products are mainly formed surrounding CH/C-S-H which will reduce the reaction rate because CO_2 has to diffuse through the product layer. Therefore, a retardant factor is added into Eq. (24) as follows:

$$k_r = (C_{Ca}^s / C_{Ca0}^s)^2 \quad (26)$$

where C_{Ca}^{s} [mol/m^3] is total concentration of solid Ca except for Ca in calcium carbonate, subscript 0 denotes the initial concentration. Finally, we obtain the following expression of the mass balance of dissolved CO_2:

$$\frac{\partial\left(\left[\phi(1-S)\frac{K_{CO_2}^{H}}{RT}+\phi S\right]c_l\right)}{\partial t}-\frac{\partial\left(\left[\frac{K_{CO_2}^{H}}{RT}v_g+v_l\right]c_l\right)}{\partial x}-\frac{\partial\left(\left[\frac{K_{CO_2}^{H}}{RT}D_g+D_l\right]\frac{\partial c_l}{\partial x}\right)}{\partial x}=-f(S)\phi k_c k_r\frac{C_{Ca}}{M_{Ca}}\frac{C_{CO_3}}{M_{CO_3}}M_{CO_2} \tag{27}$$

Each term in Eq. (27) corresponds to a different mechanism. The first term on the left hand side describes the exchanging rate of CO_2 concentration in aqueous phase. The second term is called the advection term and obeys Darcy's law. The last term involves the diffusion, following Fick's law. The right hand side of Eq. (27) is responsible for chemical reaction of CO_2 in which the total concentration of Ca^{2+} is determined by solving a separate reaction-transport Eq. of Ca^{2+} (Section 2.1.2). The initial and boundary conditions are:

$$\begin{cases} c_l(x,0)=c_{l0} & x\geq 0 \\ c_l(0,t)=c_l^{in} & t>0 \\ c_l(L,t)=c_l^{out} & t>0 \end{cases} \tag{28}$$

where c_l^{in} and c_l^{out} are the concentration of dissolved CO_2 at inlet and outlet, respectively; c_{l0} are the initial concentration of dissolved CO_2; L is the length of the sample [m]. The problem is numerically solved by using the COMSOL program.

2.1.2. Mass conservation of calcium ion

In the same way as CO_2, the mass balance equation for total Ca^{2+} is given as:

$$\partial(\phi SC_{Ca})/\partial t-\partial(v_l C_{Ca})/\partial x-\partial(D_{Ca}(\partial C_{Ca}/\partial x))/\partial x=-\phi r(M_{Ca}/M_{CO_2})+r_d \tag{29}$$

where D_{Ca} [m^2/s] is the effective diffusivity of calcium ion in the porous media (cement/concrete); r_d is the dissolution rate of CH and C-S-H [kg/m^3.s] which is calculated from the mass balance equation of total amount of Ca in solid CH and C-S-H as follows:

$$(\partial C_{Ca}^{s}/\partial t)M_{Ca}=-r_d \tag{30}$$

In order to establish a relation between concentration of calcium ion in solution and concentration of Ca in solid phases, we propose a solid-liquid equilibrium curve of Ca based on the experimental data collected by (Berner 1992) as expressed in Eq. (31).

$$C_{Ca}^{s}=\begin{cases}(d/a)C_{Ca} & C_{Ca}\leq a \\ d+((e-d)/(b-a))(C_{Ca}-a) & a<C_{Ca}\leq b \\ e+((f-e)/(c-b))(C_{Ca}-b) & b<C_{Ca}\leq c\end{cases} \tag{31}$$

The values of a, b and c are well-defined in literature. Therefore, we use fixed values: a = 2 [mol/m^3], b = 19 [mol/m^3] and c = 22 [mol/m^3] for numerical modelling. The Ca fraction in CH and C-S-H can be estimated from the hydration of minerals (C_2S, C_3S) in cement which can be estimated by the Bouge calculation. Whereas the critical value d where C-S-H starts sharply decalcifying is determined by multiplying the amount of SiO_2 in C-S-H with the corresponding Ca/Si ratio (0.85) (Berner 1992).

By substituting Eqs. (30) and (31) to Eq. (29), with initial and boundary (Neumann) conditions (32) we can determine the concentration of calcium in solution which is needed for the sink term of Eq. (27).

$$\begin{cases} C_{Ca}(x,0) = c & x \geq 0 \\ \partial C_{Ca}(0,t)/\partial x = 0 & t > 0 \\ \partial C_{Ca}(L,t)/\partial x = 0 & t > 0 \end{cases} \tag{32}$$

2.2. Derivation of auxiliary variables

2.2.1. Carbonation degree

The term "carbonation depth" is commonly used to quantify the carbonation of concrete. It is experimentally determined by the de-colouring of phenolphthalein indicator in carbonated zone. The question is how to mathematically define the carbonation depth? In the present study, we combine the carbonation reaction of CH and C-S-H. Therefore, it is logical to relate the carbonation depth to total concentration of Ca in the solid phases. Here we define the carbonation depth as the position at which X_{Ca} percentage of total Ca is carbonated. By comparing with carbonation depth determined by phenolphthalein, it is found that X_{Ca} is roughly 20%. The carbonation degree, d_c, is then formulated as:

$$d_c = \begin{cases} 1 & C_{Ca}^s < X_{Ca} f \\ (f - C_{Ca}^s)/((1 - X_{Ca}/100) f) & C_{Ca}^s \geq X_{Ca} f \end{cases} \tag{33}$$

2.2.2. Evolution of saturation degree during carbonation

As mentioned, the carbonation reactions release water. Therefore, the saturation degree (thereby RH) will change during carbonation. This change can be estimated based on the reactions of CH and C-S-H with CO_2 shown in Eqs. (16) and (17). The calculation of released water for CH carbonation is straightforward. However, for C-S-H carbonation y mol of Ca in C-S-H will release z mol H_2O. The stoichiometry values of y and z are only slightly different (Allen et al. 2007). Therefore, we assume that ratio $y/z = 1$. It is then possible to calculate the amount of released water, m_{wr} [kg], based on the change of total Ca in solid phase.

$$m_{wr} = \left(f - C_{Ca}^s\right) M_w F dx \tag{34}$$

where M_w is molar weight of water [kg/mol], F denotes surface area of sample [m^2]. The total water in domain Fdx can be computed as follows:

$$m_w = \left(f - C_{Ca}^s\right) M_w F dx + S_0 \phi_0 \gamma_w F dx \tag{35}$$

Finally, the saturation degree can be calculated as:

$$S = V_w/V_p = \left(\left(f - C_{Ca}^s\right)(M_w/\gamma_w) F dx + S_0 \phi_0 F dx\right)\Big/(\phi F dx) = \left(\left(f - C_{Ca}^s\right)(M_w/\gamma_w) + S_0 \phi_0\right)\Big/\phi \tag{36}$$

where V_w and V_p [m^3] are volumes of water and pore in domain Fdx, respectively.

2.2.3. Changes in permeability and diffusivity under saturated condition

The permeability of carbonating material varies along the depth of sample. In order to calculate the composite (or overall) permeability coefficient of the sample, the sample depth is divided into small layer Δx. The permeability of each layer is assumed to be constant. The series model is applied to calculate the composite permeability. The fluxes in each layer and the overall flux must be the same because each layer is connected together in series.

$$J_1 = J_2 = \ldots = J_n = (k_n/\eta)(\Delta p_n/\Delta x) = (k_{com}/\eta)(P/L) \tag{37}$$

where J_n, Δx and Δp_n denote the flux, thickness and pressure gradient of layer n, respectively; k_{com} denotes the composite intrinsic permeability coefficient of the sample. Additionally, the total pressure drop on each layer must be equal to gradient pressure applied on the sample. Therefore, the overall permeability can be derived as:

$$k_{com} = L \Big/ \sum_{i=1}^{n} \frac{\Delta x}{k_i} \simeq L \Big/ \int_0^L \frac{dx}{k(x)} \tag{38}$$

where $k(x)$ is intrinsic permeability at distance x. With the same approach, the composite diffusivity, D_{com} [m^2/s], of carbonated materials is written as:

$$D_{com} = L \Big/ \sum_{i=1}^{n} \frac{\Delta x}{D_i} \simeq L \Big/ \int_0^L \frac{dx}{D(x)} \tag{39}$$

where $D(x)$ [m^2/s] is effective diffusion coefficient at distance x.

3. MODELING RESULTS AND VERIFICATIONS

Experiments were performed on cement pastes with w/c ratio of 0.425. Type I ordinary Portland cement (CEM I 52.5 N) was used. Details of the setup and experimental procedure were described in (Phung et al. 2015). A pure CO_2 pressure gradient of 6 bar was applied in order to accelerate the carbonation process. A single carbonation test was performed for a period of 4 weeks.

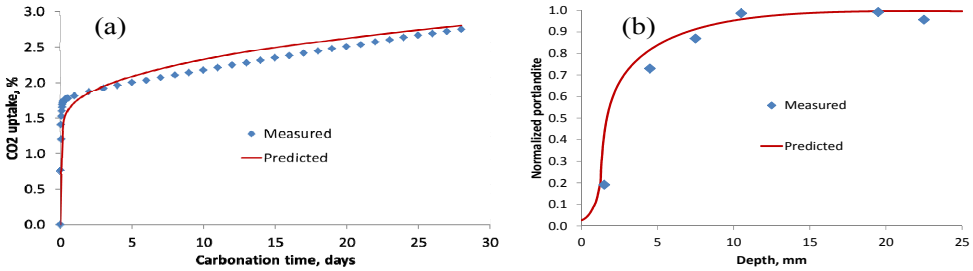

Fig. 1. CO_2 uptake (a) and portlandite profile after 28-day carbonation (b)

Fig. 1a compares the predicted CO_2 uptake with the measurement. Except for a slight difference at the transition between initial and residual stages, the predicted CO_2 uptakes are in good agreement with the measured ones. In the initial stage, CO_2 uptake rapidly increases but the uptake rate is significantly decreased in the residual stage because of porosity decrease and saturation degree increase. Fig. 1b shows the comparison of predicted portlandite profile with the one obtained by TGA measurements. The predicted value is in line with the measured one. The measured portlandite content at the downstream (not in contact with pure CO_2) is relatively smaller than the predicted value. The difference is attributed to the atmospheric carbonation which could occur during sample preparation for carbonation test or/and TGA measurements.

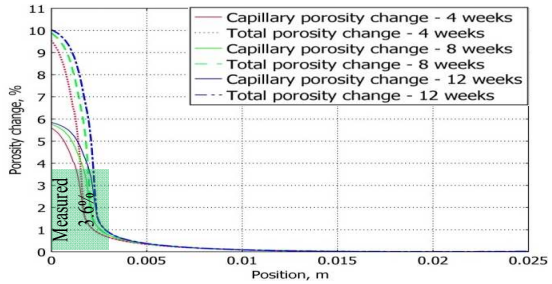

Fig. 2. Reduction of porosity (absolute value) at different carbonation time

The capillary and total porosities relatively decrease due to carbonation as shown in Fig. 2. The decrease in total porosity can mainly be attributed to the portlandite carbonation. However, in well-carbonated zone (near reacted surface), C-S-H carbonation may contribute up to 45% of

total porosity reduction. The average capillary porosity change, determined by MIP up to a depth of 3 mm from the exposed surface, compares well with the predicted capillary porosity change.

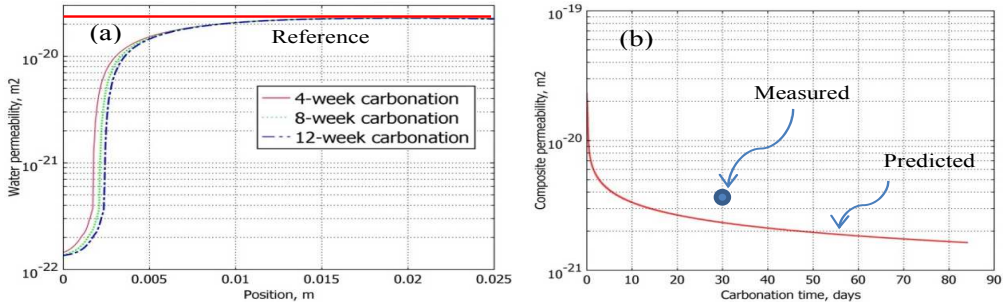

Fig. 3. Water permeability over the depth (a) and composite permeability decrease as a function of carbonation time (b)

Permeability of carbonated zone significantly decreases as shown in Fig. 3a. After 4-week carbonation, the alteration in permeability is not significant when carbonation proceeds further. The permeability coefficient decreases 2 orders of magnitude in the zone near the exposed surface. The composite permeability is dominated by the permeability of the carbonated zone despite its limited carbonation depth compared to the sample length. Therefore, a significant decrease in composite permeability is also observed as presented in Fig. 3b. The composite permeability rapidly decreases in the first few days of carbonation. It is then slightly reduced as carbonation proceeds. After 28-day carbonation, the predicted composite permeability is 2.5×10^{-21} m^2 which is a bit lower compared to the measurement (3.6×10^{-21} m^2).

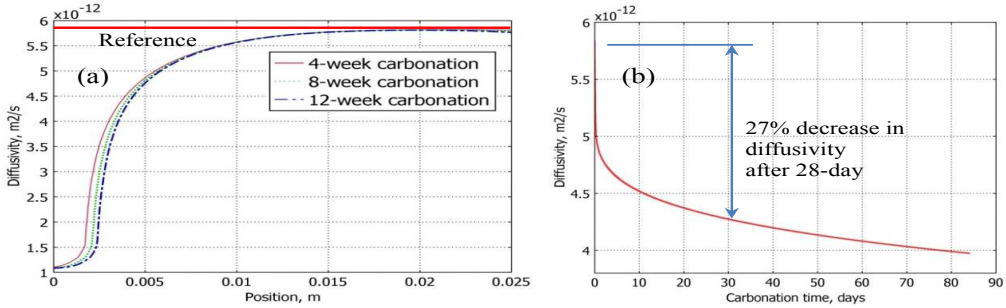

Fig. 4. Change in Ca diffusivity over the depth of at different carbonation time - (a) and composite Ca diffusivity decrease as a function of carbonation time (b)

The modification of diffusivity over the depth of sample due to carbonation is shown in Fig. 4a. The diffusivity of the carbonated zone is significantly decreased similar to the decrease in permeability. However, the magnitude of the reduction is less pronounced than for permeability. After 4 weeks of carbonation, the saturated Ca diffusivity decreases by a factor of 5 for the zone near the exposed surface which is consistent with the estimation from experimental result (4.92 times (Phung 2015)). The evolution of composite diffusivity is shown in Fig. 4b. As permeability, the composite diffusivity rapidly decreases in the first few days of carbonation. In the later stage, the diffusivity slightly decreases over carbonation time. The measured composite diffusivity of dissolved He is decreased by 30% after 28-day carbonation (Phung 2015), which is quite similar to the predicted Ca diffusivity decrease (27%). Note that the change in diffusion property of Ca and He due to carbonation may be

differed from each other because of its differences in molecular size, electrical force and binding effect.

4. CONCLUSIONS

A one-dimensional reactive transport model coupled advection and diffusion to simulate the carbonation under controlled CO_2 pressure has been developed. The model enables to predict a variety of important parameters including the CO_2 uptake, porosity change and variation of transport properties. The model helps to better interpret the experimental observations and understand the phenomena behind such as the formation of a gradual carbonation front. Primary verification with accelerated carbonation experiments gives a good agreement even though more experimental data is still required to validate and improve the model, especially to better predict the changes in transport properties.

REFERENCES

Abbas, A., Carcasses, M., and Ollivier, J. P. (1999). "Gas permeability of concrete in relation to its degree of saturation." *Mater Struct*, 32(215), 3-8.

Allen, A. J., Thomas, J. J., and Jennings, H. M. (2007). "Composition and density of nanoscale calcium-silicate-hydrate in cement." *Nat Mater*, 6(4), 311-316.

Bary, B., and Sellier, A. (2004). "Coupled moisture-carbon dioxide-calcium transfer model for carbonation of concrete." *Cement and Concrete Research*, 34(10), 1859-1872.

Berner, U. R. (1992). "Evolution of pore water chemistry during degradation of cement in a radioactive waste repository environment." *Waste Manage*, 12(2–3), 201-219.

Garboczi, E. J., and Bentz, D. P. (1992). "Computer simulation of the diffusivity of cement-based materials." *J Mater Sci*, 27(8), 2083-2092.

Glasser, F. P., Marchand, J., and Samson, E. (2008). "Durability of concrete - Degradation phenomena involving detrimental chemical reactions." *Cement and Concrete Research*, 38(2), 226-246.

Hansen, T. (1986). "Physical structure of hardened cement paste. A classical approach." *Mater Struct*, 19(6), 423-436.

Houst, Y. F., and Wittmann, F. H. (1994). "Influence of porosity and water content on the diffusivity of CO2 and O2 through hydrated cement paste." *Cement and Concrete Research*, 24(6), 1165-1176.

Morandeau, A., Thiéry, M., and Dangla, P. (2014). "Investigation of the carbonation mechanism of CH and C-S-H in terms of kinetics, microstructure changes and moisture properties." *Cement and Concrete Research*, 56(0), 153-170.

Muntean, A., Bohm, M., and Kropp, J. (2011). "Moving carbonation fronts in concrete: A moving-sharp-interface approach." *Chem Eng Sci*, 66(3), 538-547.

Papadakis, V. G., Vayenas, C. G., and Fardis, M. N. (1991). "Experimental Investigation and Mathematical-Modeling of the Concrete Carbonation Problem." *Chem Eng Sci*, 46(5-6), 1333-1338.

Papadakis, V. G., Vayenas, C. G., and Fardis, M. N. (1991). "Physical and Chemical Characteristics Affecting the Durability of Concrete." *Aci Mater J*, 88(2), 186-196.

Phung, Q. T. (2015). "Effects of Carbonation and Calcium Leaching on Microstructure and Transport Properties of Cement Pastes."PhD thesis, Ghent University, Belgium.

Phung, Q. T., Maes, N., Jacques, D., Bruneel, E., Van Driessche, I., Ye, G., and De Schutter, G. (2015). "Effect of limestone fillers on microstructure and permeability due to carbonation of cement pastes under controlled CO2 pressure conditions." *Constr Build Mater*, 82(0), 376-390.

Thiéry, M. (2005). "Modélisation de la carbonatation atmosphérique des matériaux cimentaires: prise en compte des effets cinétiques et des modifications microstructurales et hydriques."PhD thesis, Laboratoire central des ponts et chaussées, Paris.

van Genuchten, M. T. (1980). "A Closed-Form Equation for Predicting the Hydraulic Conductivity of Unsaturated Soils." *Soil Sci Soc Am J*, 44(5), 892-898.

Wardeh, G., and Perrin, B. (2006). "Relative permeabilities of cement-based materials: Influence of the tortuosity function." *J Build Phys*, 30(1), 39-57.